

Bayesian mixture modeling using a mixture of finite mixtures with normalized inverse Gaussian weights

Fumiya Iwashige and Shintaro Hashimoto
Department of Mathematics, Hiroshima University

December 25, 2025

Abstract

In Bayesian inference for mixture models with an unknown number of components, a finite mixture model is usually employed that assumes prior distributions for mixing weights and the number of components. This model is called a mixture of finite mixtures (MFM). As a prior distribution for the weights, a (symmetric) Dirichlet distribution is widely used for conjugacy and computational simplicity, while the selection of the concentration parameter influences the estimate of the number of components. In this paper, we focus on estimating the number of components. As a robust alternative Dirichlet weights, we present a method based on a mixture of finite mixtures with normalized inverse Gaussian weights. The motivation is similar to the use of normalized inverse Gaussian processes instead of Dirichlet processes for infinite mixture modeling. Introducing latent variables, the posterior computation is carried out using block Gibbs sampling without using the reversible jump algorithm. The performance of the proposed method is illustrated through some numerical experiments and real data examples, including clustering, density estimation, and community detection.

Keywords: Bayesian nonparametrics; Clustering; Dirichlet distribution; Inverse Gaussian distribution; Markov chain Monte Carlo; Mixture models

1 Introduction

We consider a finite mixture model with an unknown number of components:

$$f(y \mid \theta_1, \dots, \theta_M, \pi) = \sum_{j=1}^M \pi_j f(y \mid \theta_j), \quad (1.1)$$

where $M \in \{1, 2, \dots\}$ is the number of components, $y \in \mathbb{R}^d$ is a d -dimensional observation vector, and $\pi = (\pi_1, \dots, \pi_M)^\top$ is the mixing weight vector, satisfying $\sum_{j=1}^M \pi_j = 1$ and $\pi_j > 0$. For $j = 1, \dots, M$, $f(\cdot \mid \theta_j)$ is a probability density or probability mass function parameterized by the component-specific parameter θ_j . The function $f(\cdot \mid \theta_j)$ is also called the kernel of the mixture model. Each observation is assumed to arise from one of the M components, and each component is weighted based on its frequency of occurrence. Mixture models are important statistical models used in model-based clustering and density estimation because they can model complex data-generating distributions in random phenomena by using multiple components. Finite mixture models have been applied in many fields, for instance, sociology (Handcock et al., 2007), economics (Frühwirth-Schnatter and Kaufmann, 2008) and genetics (McLachlan et al., 2002) and so on. In applications, the determination of M is a very important issue. Correctly estimating M improves model interpretability, the accuracy of kernel parameter estimates and model predictions, and reduces computation time. Although various methods have been proposed for the selection of M , such as model selection criteria and hypothesis testing, using these criteria make it difficult to quantify the uncertainty of M , and also introduces the bias that model selection is carried out. A comprehensive review of (finite) mixture models is provided by McLachlan (2000); Frühwirth-Schnatter (2006); Frühwirth-Schnatter et al. (2019); McLachlan et al. (2019). In this paper, we focus on the case where M is finite and make a clear distinction between the number of components M and the number of clusters k . In general, the number of components is written as $M = k + M_{na}$, where k is the number of components for which data are actually assigned, and M_{na} is the number of empty components (see also Argiento and De Iorio, 2022).

Although we also estimate M in this paper, there are two important issues associated

with its inference. First, for any finite data set, M is not a well-defined quantity and cannot be directly inferred from the data. In certain application domains of mixture models, such as species sampling in biology (see e.g., Argiento et al., 2014), it is even expected that data from some components may not be observed at all. Thus, given the data, we can only make predictions about M , and the prior on M and the prior on the weight distribution play a crucial role. Second, the posterior distribution of M is highly sensitive to model misspecification. Most consistency results for M are derived under the assumption of model correctness (Nobile, 1994; Miller, 2023). Therefore, when attempting to infer the number of mixture components, it is critically important to ensure that the data-generating process is appropriately captured.

In Bayesian analysis, a finite mixture model that assumes prior distributions for the mixing weights and the number of components is usually employed (see, e.g. Nobile, 1994; Miller and Harrison, 2018). Such a model is also called a mixture of finite mixtures (MFM), and the model is often used, as well as infinite mixture models represented by Dirichlet process mixture models. Although the reversible jump algorithm (Green, 1995; Richardson and Green, 1997) has been used to obtain samples from the posterior distribution based on MFM, it faces significant computational and implementation challenges. Methods based on marginal likelihoods have also been proposed (see, e.g. Nobile and Fearnside, 2007), while, as with reversible jump, the computational aspect is an issue. Recently, the use of nonparametric Bayesian methods for MFM to estimate M has attracted much attention. In Miller and Harrison (2018), the exchangeable partition distribution is derived by marginalizing out M , and the restaurant process is constructed to overcome computational difficulties. Note that the result of Miller and Harrison (2018) has some connection with Pitman-Yor process prior (see e.g. Section 4.1 in Frühwirth-Schnatter et al. (2021)). In Frühwirth-Schnatter et al. (2021), a generalized MFM in which the parameters of the Dirichlet distribution depend on M is proposed. They showed that this model class may be regarded as a Bayesian nonparametric mixture outside the class of Gibbs-type priors, and proposed a novel sampling algorithm so-called telescoping sampling. In Argiento and De Iorio (2022), they developed an MFM framework based on a

nonparametric Bayesian prior, the normalized independent finite point process. By introducing a gamma latent variable, their approach encompasses a broad class of distributions on the simplex and yields an efficient blocked Gibbs sampling derived from the posterior random measure.

Most studies on MFMs employ a (symmetric) Dirichlet distribution for the mixing weights because of its analytical convenience. Argiento and De Iorio (2022) primarily consider not only the Dirichlet distribution but also a family of simplex distributions constructed from σ -stable laws. However, the σ -stable example is treated as a central case, since their paper emphasizes that a restaurant process based computational algorithm can be constructed whenever the Laplace transform of the weight distribution is available.

In this paper, we study a new MFM based on the normalized inverse Gaussian distribution, building on the results of Argiento and De Iorio (2022). We compare the proposed MFM with the MFM on the Dirichlet prior, focusing on the distributional differences from the Dirichlet case. To the best of our knowledge, there are few studies using the normalized inverse Gaussian distributions as the mixing weights in the field of finite mixture models. In Bayesian nonparametric inference with infinite mixtures, Lijoi et al. (2005) proposed a normalized inverse Gaussian process and showed some analytical results of the posterior distribution under the process. Furthermore, we clarify the relationship between the blocked Gibbs sampling and the telescoping sampling, and extend the telescoping sampling so that it can be applied to general distributions on the simplex.

This paper is organized as follows. In Section 2, we provide a brief review of MFMs and its equivalent representation using discrete probability measures. We also discuss the data augmentation and the conditional posterior distribution of M_{na} , which are crucial for constructing the computational algorithm. In Section 3, we present the proposal method as well as the posterior computation algorithm. In Section 4, we illustrate some numerical studies to compare the proposed method with existing methods. R code implementing the proposed methods is available at Github repository:

<https://github.com/Fumiya-Iwashige/MFM-Inv-Ga>

2 Mixture of finite mixtures

We present a brief overview of a MFM and its equivalent representation of the discrete probability measure. The proposed model and the posterior computation algorithm presented in the next section are largely based on the basic model presented in this section.

2.1 Formulation

Let each observation Y_1, \dots, Y_n be univariate or multivariate in a Euclidean space. An MFM is a statistical model defined by the following hierarchical representation.

$$\begin{aligned}
 M - 1 &\sim q_M, \quad q_M \text{ is a probability mass function (p.m.f.) on } \{0, 1, 2, \dots\}, \\
 \pi \mid M &\sim P_\pi(\pi \mid M), \\
 c_i \mid M, \pi &\sim \text{Categorical}_M(\pi), \quad i = 1, \dots, n, \\
 \tau_m \mid M &\stackrel{\text{i.i.d.}}{\sim} p_0(\tau), \quad m = 1, \dots, M, \\
 \theta_i \mid c_i, \tau_{1:M} &\stackrel{\text{ind}}{\sim} \delta_{\tau_{c_i}}(\theta_i), \quad i = 1, \dots, n, \\
 Y_i \mid \theta_i &\stackrel{\text{ind}}{\sim} f(y_i \mid \theta_i), \quad i = 1, \dots, n,
 \end{aligned} \tag{2.1}$$

where $f(y \mid \theta_i)$ is a parametric model with parameter θ_i , $\delta_x(\cdot)$ is a point mass at x and τ_m is an element of a vector $\tau_{1:M} = (\tau_1, \dots, \tau_M)^\top$. $p_0(\tau_{1:M})$ is a prior density function of the parameter in mixture components. The parameter space is denoted by $\Theta \subset \mathbb{R}^d$. Each c_i is a latent allocation indicates to which component each observation is allocated. Given the number of components M , $P_\pi(\pi \mid M)$ is a probability distribution on the M -dimensional unit simplex, in that, this is the prior distribution for the mixing weights.

Let h be a probability density function (p.d.f) on \mathbb{R}_+ . We focus on the case where the mixing weights can be further hierarchically expressed as follows:

$$\begin{aligned}
 S_m \mid M &\stackrel{\text{ind}}{\sim} h, \\
 \pi &= \left(\frac{S_1}{T}, \dots, \frac{S_M}{T} \right) \sim P_\pi(\pi \mid M), \quad T = \sum_{m=1}^M S_m,
 \end{aligned} \tag{2.2}$$

where S_1, \dots, S_M are unnormalized weights and π is (normalized) mixing weight vector.

This representation is the most basic way to generate a probability distribution on the d -dimensional unit simplex $\mathbb{S}_d := \{w = (w_1, \dots, w_d); w_i \geq 0, \sum_{i=1}^d w_i = 1\}$. One of the most famous examples of a distribution on \mathbb{S}_d is the Dirichlet distribution. If $S_i \sim \text{Gamma}(\gamma_i, 1)$ in (2.2), $\pi \sim \text{Dirichlet}(\gamma_1, \dots, \gamma_d)$, where $\text{Gamma}(a, b)$ is the gamma distribution with shape parameter $a > 0$ and rate parameter $b > 0$, and $\text{Dirichlet}(\gamma_1, \dots, \gamma_d)$ is the Dirichlet distribution with parameter $(\gamma_1, \dots, \gamma_d)$. When we set $\gamma_1 = \dots = \gamma_d (= \gamma > 0)$, we have the symmetric Dirichlet distribution $\text{Dirichlet}(\gamma, \dots, \gamma)$, and this distribution is often used as a prior distribution for mixing weight vector in the framework of MFM, because of conjugacy with categorical distributions and simplicity of computation. The symmetric structure of $\text{Dirichlet}(\gamma, \dots, \gamma)$ is also essential for marginalizing out M and deriving the exchangeable partition probability function (EPPF).

Also, if the hyperparameters of h depend on M in (2.2), the model is referred to as a generalized MFM:

$$S_m | M \stackrel{\text{ind}}{\sim} h_M, \quad m = 1, \dots, M, \quad (2.3)$$

$$\pi = \left(\frac{S_1}{T}, \dots, \frac{S_M}{T} \right) \sim P_\pi(\pi | M), \quad T = \sum_{m=1}^M S_m.$$

In particular, if the shape parameters are divided by M , the model is referred to as a *dynamic* MFM (DMFM). The Dirichlet case, where h_M is $\text{Gamma}(\gamma/M, 1)$, is discussed in Frühwirth-Schnatter et al. (2021). On the other hand, Frühwirth-Schnatter et al. (2021) referred to MFM defined by (2.1), in which the distributional parameters of S_m do not depend on M , as *static* MFM. In this paper, we simply refer to such static MFM as MFM.

However, it is known that the estimation result is sensitive to the choice of the shape parameter γ . For example, Miller and Harrison (2018) recommended to use $\gamma = 1$ as a default choice and the value works well in many cases. On the other hand, in the sparse MFM, dividing by a large M effectively corresponds to using a small value of γ . Moreover, because γ strongly influences both the prior distribution of the number of clusters and the induced partition distribution, it is necessary to assign an appropriate prior to γ . For further discussion of broader prior specifications, see Greve et al. (2022).

2.2 Equivalent representations using discrete probability measures

Following Argiento and De Iorio (2022), we give an equivalent representation of the MFM. We can construct a discrete measure $P(\cdot) = \sum_{m=1}^M \pi_m \delta_{\tau_m}(\cdot)$ in the parameter space Θ , almost surely, where M , τ and π are realizations from the distributions q_M , p_0 and P_π , respectively. Let $\theta_1, \dots, \theta_n$ be random variables according to P . Then, the model (2.1) is equivalent to the following hierarchical representation using a random measure P .

$$\begin{aligned} Y_i | \theta_i &\stackrel{\text{i.i.d.}}{\sim} f(y_i | \theta_i), \quad i = 1, \dots, n, \\ \theta_1, \dots, \theta_n | P &\stackrel{\text{i.i.d.}}{\sim} P, \\ P &\sim \mathcal{P}(q_M, h, p_0), \end{aligned} \tag{2.4}$$

where \mathcal{P} is a probability distribution of P with parameters q_M , h and p_0 . The representation (2.4) is the MFM described in the same framework as infinite mixtures. If we replace \mathcal{P} with the Dirichlet process, (2.4) represents the well-known Dirichlet process mixture models (e.g., Escobar and West, 1995). If we replace \mathcal{P} with the normalized inverse Gaussian process, (2.4) represents the normalized inverse Gaussian process mixture models (Lijoi et al., 2005). For MFMs, Argiento and De Iorio (2022) proposed a normalized independent finite point process (Norm-IFPP), which is a class of flexible prior distributions for P . We employ the representation (2.4) with the Norm-IFPP. The advantages are as follows. We can directly estimate M and k . Furthermore, an efficient Gibbs sampler can be constructed by incorporating the data augmentation with a latent Gamma random variable. This data augmentation enables us to overcome the lack of conjugacy in the categorical distribution. Instead of using the probability density function of P_π , we can use the density function of h . This is the key to building an efficient MCMC algorithm for the proposed model. The details of Norm-IFPP and the independent finite point process (IFPP) are given in Argiento and De Iorio (2022).

2.3 Data augmentation and conditional distribution of M_{na}

We illustrate the data augmentation and conditional posterior distribution of M_{na} . We introduce the data augmentation in models (2.1) and (2.2). This technique is employed in James et al. (2009) and Argiento and De Iorio (2022). Let \mathcal{M}_a and \mathcal{M}_{na} be the allocated and unallocated index sets, respectively. The conditional joint distribution of $\tau = (\tau_1, \dots, \tau_M)^\top$ and $S = (S_1, \dots, S_M)^\top$ given M and a label vector c is

$$\begin{aligned} p(S, \tau \mid M, c) &\propto \left(\prod_{i=1}^n \frac{S_{c_i}}{T} \right) \left(\prod_{m=1}^M h(S_m) p(\tau_m) \right) \\ &= \left(\prod_{m \in \mathcal{M}_a} \left(\frac{S_m}{T} \right)^{n_m} h(S_m) p(\tau_m) \right) \left(\prod_{m \in \mathcal{M}_{na}} h(S_m) p(\tau_m) \right), \end{aligned}$$

where $n_m = \#\{i : c_i = m\}$ and $T = \sum_{m=1}^M S_m$, which depends on S . Furthermore, using $U_n \mid T \sim \text{Gamma}(n, T)$, we obtain

$$p(S, \tau, U_n \mid M, c) \propto u^{n-1} \left(\prod_{m \in \mathcal{M}_a} e^{-S_m U_n} S_m^{n_m} h(S_m) p(\tau_m) \right) \left(\prod_{m \in \mathcal{M}_{na}} e^{-S_m U_n} h(S_m) p(\tau_m) \right).$$

Thus, the conditional distribution of each S_m is

$$S_m \mid U_n = u, M = m, c \stackrel{\text{i.i.d.}}{\sim} e^{-S_m u} S_m^{n_m} h(S_m), \quad m \in \mathcal{M}_a, \quad (2.5)$$

$$S_m \mid U_n = u, M = m, c \stackrel{\text{i.i.d.}}{\sim} e^{-S_m u} h(S_m), \quad m \in \mathcal{M}_{na}. \quad (2.6)$$

If it is easy to generate random variables from the distributions in (2.5) and (2.6), an efficient Gibbs sampling algorithm can be constructed. For example, when the prior distribution of the unnormalized weight is an inverse Gaussian distribution, (2.5) and (2.6) are generalized inverse Gaussian distributions. Introducing U_n , the update of the variable π is replaced by the update of the variable S_m . Thus, the selection of h is essential in MCMC updates.

Under this data augmentation, the conditional distribution of M_{na} is established in Theorem 5.1 in Argiento and De Iorio (2022). This theorem states that if $\mathcal{P}(q_M, h, p_0)$ follows a Norm-IFPP, then the posterior distribution of the random measure P , given

U_n , is a superposition of a finite point process with fixed points and an IFPP. The IFPP characterizes the process of unallocated jumps, where the discrete probability distribution that serves as its parameter corresponds to the distribution of M_{na} . The conditional distribution of M_{na} is given by

$$\mathbb{P}(M_{na} = m \mid \theta, U_n = u, k) \propto \frac{(m+k)!}{m!} \psi(u)^m q_M(m+k), \quad m = 1, 2, \dots, \quad (2.7)$$

where $\theta = (\theta_1, \dots, \theta_n)^\top$, k is the number of clusters (unique values of θ) and ψ is the Laplace transform of h . We sample M_{na} from (2.7) in the MCMC algorithm. Then, we straightforwardly obtain M by adding k to M_{na} .

3 Methodology

In this section, we propose a mixture of finite mixtures with normalized inverse Gaussian weights. The posterior inference based on the proposed model can be efficiently implemented using the blocked Gibbs sampling proposed by Argiento and De Iorio (2022).

3.1 Mixture of finite mixtures with normalized inverse Gaussian weights

We propose a mixture of finite mixtures with normalized inverse Gaussian weights (denoted by MFM-IGau), where the notation explicitly specifies h because it is essential for computation. Our proposal model only requires (2.2) to be

$$S_m \mid M \stackrel{\text{ind}}{\sim} \text{IGau}(\alpha, 1), \quad \alpha > 0,$$

$$\pi = \left(\frac{S_1}{T}, \dots, \frac{S_M}{T} \right) \sim \text{NIGau}(\alpha, \dots, \alpha),$$

where $\text{IGau}(\alpha, \beta)$ is the inverse Gaussian distribution with shape parameter $\alpha > 0$ and scale parameter $\beta > 0$, and $\text{NIGau}(\alpha_1, \dots, \alpha_d)$ is the normalized inverse Gaussian distribution with parameters $\alpha_i > 0$ for $i = 1, \dots, d$. The probability density function of a

random variable S according to $\text{IGau}(\alpha, \beta)$ is given by

$$h(s) = \frac{\alpha}{\sqrt{2\pi}} s^{-3/2} \exp\left(-\frac{1}{2} \left(\frac{\alpha^2}{s} + \beta^2 s\right) + \beta\alpha\right), \quad s > 0, \quad (3.1)$$

where $\alpha > 0$ is the shape parameter and $\beta > 0$ is the scale parameter. The mean and variance of S are given by

$$\mathbb{E}[S] = \frac{\alpha}{\beta}, \quad \text{Var}[S] = \frac{\alpha}{\beta^3}. \quad (3.2)$$

Let $\psi_{\text{IGau}}(u)$ be the Laplace transforms of $\text{IGau}(\alpha, 1)$. $\psi_{\text{IGau}}(u)$ is the following:

$$\psi_{\text{IGau}}(u) = \exp\left(\alpha \left(1 - \sqrt{1 + 2u}\right)\right), \quad u \geq 0. \quad (3.3)$$

Also, cumulant $\kappa_{\text{IGau}}(n, u) := (-1)^n \frac{d^n}{du^n} \psi_{\text{IGau}}(u)$ is

$$\kappa_{\text{IGau}}(u; n) = \alpha^n \psi_{\text{IGau}}(u) (1 + 2u)^{-n/2} \frac{K_{n-1/2}(\alpha\sqrt{1+2u})}{K_{1/2}(\alpha\sqrt{1+2u})}, \quad (3.4)$$

where K_m is the modified Bessel functions of the second kind of order m . The derivation of (3.4) is provided in the Supplementary Material. From Lijoi et al. (2005), the probability density function of the normalized inverse Gaussian distribution with parameters $\alpha_i > 0$, $i = 1, \dots, d$ is given by

$$f(\pi) = \frac{e^{\sum_{i=1}^d \alpha_i} \prod_{i=1}^d \alpha_i}{2^{d/2-1} \pi^{d/2}} \times K_{-d/2}\left(\sqrt{\mathcal{A}_d(\pi_1, \dots, \pi_{d-1})}\right) \times \left(\pi_1^{3/2} \dots \pi_{d-1}^{3/2} \left(1 - \sum_{i=1}^{d-1} \pi_i\right)^{3/2} \times \mathcal{A}_d(\pi_1, \dots, \pi_{d-1})^{d/4}\right)^{-1}, \quad (3.5)$$

where $\mathcal{A}_d(\pi_1, \dots, \pi_{d-1}) = \sum_{i=1}^{d-1} \alpha_i^2 / \pi_i + \alpha_d^2 \left(1 - \sum_{i=1}^{d-1} \pi_i\right)^{-1}$.

The normalized inverse Gaussian distribution is less informative and more robust to parameter specification than the Dirichlet distribution. In the context of DMFM, shape parameters such as γ/M or α/M become small, and information measures such as entropy and the Gini index of $\text{Dirichlet}(\gamma/M, \dots, \gamma/M)$ also tends to be very small. Therefore,

it is desirable to incorporate learning for γ . In contrast, those of $\text{NIGau}(\alpha/M, \dots, \alpha/M)$ does not decrease as easily, so stable posterior inference can be achieved regardless of the choice of α . This fact is confirmed through the numerical experiment in Section 4.1.1. Further analysis of the Gini index is provided in the Supplemental Material. Also, in the context of infinite mixtures, it is known that the prior on the number of clusters induced by the normalized inverse Gaussian process has heavier tails than that induced by the Dirichlet process (Lijoi et al., 2005). It is expected that this robustness carries over to the finite mixture setting as well. These provide the main motivations for using the normalized inverse Gaussian distribution as mixing weights.

Due to the breakdown of conjugacy with the categorical distribution, constructing an efficient Gibbs sampler is challenging. Because of the complexity of (3.5), the calculation in Miller and Harrison (2018) is intractable: constructing MCMC algorithm based on the restaurant process by marginalizing out M is extremely challenging. To overcome this difficulty, we use the data augmentation technique and the sampling method proposed by Argiento and De Iorio (2022). As a result, it is no longer necessary to deal directly with the normalized inverse Gaussian distribution (3.5), and the simple MCMC algorithm can be constructed using only the inverse Gaussian distribution (3.1) and its Laplace transform.

3.2 Posterior computation

In this section, we present a fast and efficient posterior computation algorithm for the proposed method. To this end, we adopt the blocked Gibbs sampling scheme in Argiento and De Iorio (2022). Moreover, we discuss the blocked Gibbs sampling in detail and explain the computational advantages of using inverse Gaussian weights.

Let η and ρ be hyperparameters of q_M and h , respectively, and $p(\cdot)$ be a joint prior density function except for h and q_M . $n_m = \#\{i; c_i = m\}$ is the size of the m th cluster. $\psi(u)$ is the Laplace transform of h , which is defined by $\psi(u) := \mathbb{E}[e^{-uS_m}]$ for $u \geq 0$. $\kappa(u; n)$ is the cumulant of h , which is defined by $\kappa(u; n) := (-1)^n \frac{d^n}{du^n} \psi(u)$. Note that $\psi(u)$ and $\kappa(u; n)$ depend on ρ .

We summarize the algorithm in Algorithm 1. The point of this algorithm is the data

Algorithm 1 blocked Gibbs sampling (Argiento and De Iorio, 2022)

Step 0. Set initial values.

Step 1. Sample U_n from $\text{Gamma}(n, T)$, where $T = \sum_{m=1}^M S_m$.

Step 2. Sample c_i , for $i = 1, \dots, n$ from the following discrete probability distribution defined by each probability

$$\mathbb{P}(c_i = j \mid \text{rest}) \propto S_j f(y_i \mid \tau_j), \quad j = 1, \dots, M.$$

Step 3. Sample the hyperparameter η of the q_M from

$$p(\eta \mid \text{rest}) \propto \Psi(u, k) p(\eta), \quad \Psi(u, k) := \sum_{m=0}^{\infty} \frac{(m+k)!}{m!} \psi(u)^m q_M(m+k).$$

Step 3'. Sample the hyperparameter ρ of the h from

$$p(\rho \mid \text{rest}) \propto \Psi(u, k) \prod_{j=1}^k \kappa(u; n_j) p(\rho).$$

Step 4. Sample M_{na} from the following discrete distribution

$$\mathbb{P}(M_{na} = m \mid \text{rest}) \propto \frac{(m+k)!}{m!} \psi(u)^m q_M(m+k), \quad m = 0, 1, \dots$$

Step 5. Sample S_m , for $m = 1, \dots, k$ from $e^{-S_m u} S_m^{n_m} h(S_m)$.

Step 6. Sample τ_m , for $m = 1, \dots, k$ from

$$p(\tau_m \mid \text{rest}) \propto \left\{ \prod_{i; \theta_i = \tau_m} f(y_i \mid \tau_m) \right\} p(\tau).$$

Step 7. Sample $S_{m_{na}}$, for $m_{na} = k+1, \dots, M_{na} + k$ from $e^{-S_{m_{na}} u} h(S_{m_{na}})$.

Step 8. Sample $\tau_{m_{na}}$, for $m_{na} = k+1, \dots, M_{na} + k$ from the prior $p(\tau)$.

augmentation through the latent variable such as $U_n \mid T \sim \text{Gamma}(n, T)$, where n is the sample size and $T = \sum_{m=1}^M S_m$. It is important to sample the number of empty components M_{na} from (2.7) in Step 4. This step allows for direct sampling of M by adding k and label variables to be updated as in the finite mixture model with given M in step 2. The update is the same as the telescoping sampling proposed by Frühwirth-Schnatter et al. (2021), and the method is more efficient than the classical restaurant process. However, in implementation, it is important to determine q_M so that the series $\Psi(u, k)$ in Steps 3 and 4 can be written analytically and random variables can be easily generated from the full conditional distributions of η and M_{na} . In Step 5 and 7, the allocated and unallocated weights are updated based on (2.5) and (2.6), respectively. The

prior h of S_m is discussed in detail in the next paragraph. In Steps 7, 8, the assigned unnormalized weights and kernel parameters are updated. When M_{na} sampled in Step 4 is greater than or equal to 1, Steps 7 and 8 are executed.

To implement the blocked Gibbs sampling, at least two conditions must be satisfied: 1) both the probability density function and the Laplace transform must be available in closed form, 2) each S_m can be easily generated from (2.5) and (2.6). Additionally, it is desirable that the cumulants of h can be expressed in closed form when updating η or when extending the (static) MFM to the DMFM. When S_m follows the σ -stable distribution, the blocked Gibbs sampling, in general, cannot be used, as the probability density function is available in integral form. Alternatively, a marginal Gibbs sampler based on the restaurant process is required, as employed in Argiento and De Iorio (2022).

The inverse Gaussian distribution satisfies all of the conditions. The probability distribution, the Laplace transform and the cumulant are given by (3.1), (3.3) and (3.4) respectively. If h is the IGau($\alpha, 1$), the full conditional distribution of S_m is the generalized inverse Gaussian distribution. From (2.5) and (2.6), we have

$$S_m \mid U_n = u, M = m, c \stackrel{\text{i.i.d}}{\sim} \text{GIG}(2u + 1, \alpha^2, n_m - 1/2), \quad m \in \mathcal{M}_a,$$

$$S_m \mid U_n = u, M = m, c \stackrel{\text{i.i.d}}{\sim} \text{GIG}(2u + 1, \alpha^2, -1/2), \quad m \in \mathcal{M}_{na},$$

where GIG(a, b, c) is the generalized inverse Gaussian distribution with $a > 0, b > 0, c \in \mathbb{R}$.

3.3 Prior distributions for the number of mixture components

Assume that $M-1$ follows a discrete probability distribution with the support $\{0, 1, 2, \dots\}$. In this paper, we consider Poisson(Λ) ($\Lambda > 0$) for $M-1$, because the constraints in Steps 3 and 4 are satisfied. In fact, from Argiento and De Iorio (2022), we have

$$\Psi(u, k) = \Lambda^{k-1}(\Lambda\psi(u) + k) \exp(\Lambda(\psi(u) - 1)). \quad (3.6)$$

Assuming $\Lambda \sim \text{Gamma}(a_\Lambda, b_\Lambda)$ for $a_\Lambda, b_\Lambda > 0$, the full conditional distributions of Λ and M_{na} are given by

$$\begin{aligned} p(\Lambda \mid \text{rest}) &\propto \psi(u)(k + a_\Lambda - 1)\text{Gamma}(k + a_\Lambda + 1, 1 - \psi(u) + b_\Lambda) \\ &\quad + k(b_\Lambda + 1 - \psi(u))\text{Gamma}(k + a_\Lambda, 1 - \psi(u) + b_\Lambda), \\ \mathbb{P}(M_{na} = m \mid \text{rest}) &\propto \Lambda\psi(u)\text{Shifted-Poisson}(\Lambda\psi(u), 1) + k\text{Poisson}(\Lambda\psi(u)), \end{aligned}$$

respectively, where $\text{Shifted-Poisson}(\Lambda, t)$ is parallel shifted of the distribution $\text{Poisson}(\Lambda)$ by t . Furthermore, if b_Λ is hierarchically assigned a beta-prime prior $\text{Betaprime}(a_p, b_p)$, $a_p, b_p > 0$, then the marginal prior of $M-1$ follows a beta-negative binomial distribution $\text{BNB}(a_\Lambda, a_p, b_p)$. Frühwirth-Schnatter et al. (2021) recommend using $\text{BNB}(1, 4, 3)$ under Dirichlet weights. It should be noted, however, that updating b_Λ requires the Metropolis–Hastings algorithm. Therefore, various discrete distributions can be incorporated into the prior for $M-1$ by using a Poisson-based hierarchical structure.

3.4 Specification of kernels

The choice of kernel is important, and the appropriate kernel must be selected for the purpose. In this paper, although we do not discuss the details of the selection of kernels, we present some famous kernels for the sake of completeness.

3.4.1 Cluster analysis and density estimation

One of the most famous and useful kernels is the (multivariate) normal kernel $N(y \mid \mu, \sigma^2)$. In the univariate case, we often use the normal inverse gamma model as a prior distribution of $\tau = (\mu, \sigma^2)$: $\mu \mid \sigma^2 \sim N(m_0, \sigma^2/\eta)$, $\sigma^2 \sim \text{IG}(c_0, C_0)$, where $m_0 \in \mathbb{R}$, $\eta, c_0, C_0 > 0$. The parameter η is called a smoothing parameter and plays an important role in density estimation. It is possible to include a hierarchical prior for η . In the multivariate case, the hierarchical normal inverse Wishart model: $\mu \sim N_r(b_0, B_0), \Sigma^{-1} \mid C \sim W(c_0, C), C \sim W(g_0, G_0)$, where $b_0 \in \mathbb{R}^r$, B_0 is an $r \times r$ covariance matrix, $c_0, g_0 > r - 1$, and G_0 is an $r \times r$ positive definite symmetric matrix. We used normal kernels in later numerical

experiments in Sections 4.1 and 4.2 for clustering and density estimation. Of course, other kernels can also be used depending on the purpose (see e.g., Frühwirth-Schnatter and Pyne, 2010).

3.4.2 Network analysis

As an application of the proposed method, we perform community detection on network data. Community detection is the task of identifying dense subclasses in network data, corresponds to clustering and estimating the number of components, called the number of communities in network analysis. Note that the number of components of finite mixture models is equivalent to the number of communities in the network, and both are denoted M . Estimating the number of communities is an important problem and various methods have been proposed (Shi and Malik, 2000; Newman, 2004; White and Smyth, 2005). From a model-based perspective, it is essentially the same as estimating the number of components in a finite mixture model, and we can apply MFM. The stochastic block model is a famous statistical model of network data (Holland et al., 1983), which assumes a stochastic block structure behind and specifies the community structure by estimating the probability of edges being drawn between each group. Geng et al. (2019) proposed a stochastic block model based on MFM with Dirichlet weights, and also constructed a similar algorithm to Miller and Harrison (2018).

MFM can be easily applied to community detection by modifying the kernel. Data y are replaced by the adjacency matrix $A \in \mathbb{R}^{n \times n}$, where $A = (A_{ij}) \in \{0, 1\}^{n \times n}$ and n is the number of the node. When $A_{ij} = 1$, this indicates that an edge is drawn from the i th node to the j th node, and when $A_{ij} = 0$, this does not. For simplicity, we assume that the adjacency matrix is not directed and does not have a self-loop, in that $A_{ij} = A_{ji}$ and $A_{ii} = 0$, where $1 \leq i < j \leq n$. The stochastic block model is formulated as follows,

$$\begin{aligned} A_{ij} \mid Q, M &\sim \text{Bernoulli}(\theta_{ij}), \quad \theta_{ij} = Q_{c_i c_j}, \quad 1 \leq i < j \leq n, \\ Q_{rs} &\sim \text{Beta}(a_Q, b_Q), \quad 1 \leq r \leq s \leq M, \end{aligned} \tag{3.7}$$

where $a_Q, b_Q > 0$ and M is the number of communities. $Q = (Q_{rs}) \in [0, 1]^{M \times M}$ is a

symmetric matrix and defines the stochastic block structure of a network. Each element Q_{rs} represents the probability that an edge is drawn between any node belonging to the community label r and any node belonging to the community label s . To perform community detection for the proposed model, we just set the Bernoulli likelihood as the kernel.

3.5 Evaluation of the number of empty components

For the full conditional distribution of M_{na} , the following inequality holds, where $M - 1 \mid \Lambda \sim \text{Poisson}(\Lambda)$ and $\Lambda \sim \text{Gamma}(a_\Lambda, b_\Lambda)$ for $a_\Lambda, b_\Lambda > 0$.

Proposition 3.1. *For the full conditional distribution of M_{na} , the inequalities*

$$\mathbb{P}(M_{na} \geq 1 \mid U_n = u, k, \Lambda) \leq \Lambda \psi(u) \left(1 + \frac{1}{\Lambda \psi(u) + k} \right), \quad (3.8)$$

$$\mathbb{P}(M_{na} \geq 1 \mid U_n = u, k) \leq \psi(u) \frac{a_\Lambda}{b_\Lambda} \left(1 + \frac{1}{k} \right) \quad (3.9)$$

hold, where ψ is the Laplace transform of the density h .

The proof of the proposition is given in the Supplementary Material. Proposition 3.1 shows that $\psi(u)$ plays an important role in generating empty components. The critical difference between the inverse Gaussian and gamma distributions is the Laplace transform. Let $\psi_{\text{Gamma}}(u)$ be the Laplace transforms of $\text{Gamma}(\gamma, 1)$:

$$\psi_{\text{Gamma}}(u) = \left(\frac{1}{1+u} \right)^\gamma, \quad u \geq 0. \quad (3.10)$$

Laplace transforms ψ_{IGau} and ψ_{Gamma} are decreasing functions with respect to u . The former has exponential decay, while the latter is polynomial. Figure 1 shows the graphs of the Laplace transforms of inverse Gaussian and gamma distributions when the shape parameters are $\alpha, \gamma = 1.0, 0.2, 10^{-1}, 10^{-2}, 10^{-3}$ and the scale parameters are 1. It can be seen that ψ_{IGau} decreases much faster than ψ_{Gamma} , contributing to the suppression of M_{na} .

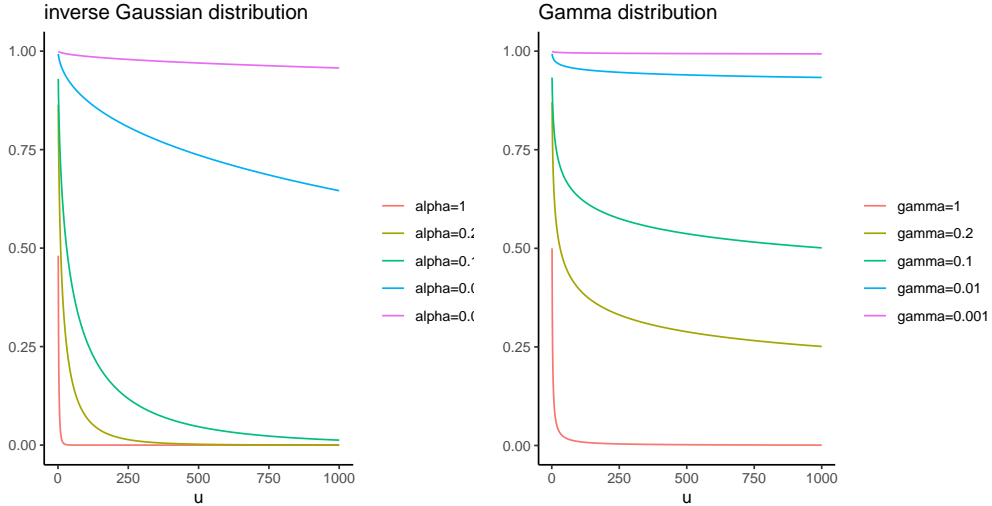


Figure 1: When shape parameters are $\alpha = \gamma = 1, 0.2, 10^{-1}, 10^{-2}, 10^{-3}$, left graphs are Laplace transforms of $\text{IGau}(\alpha, 1)$, right graphs are Laplace transforms of $\text{Gamma}(\gamma, 1)$.

Inequalities (3.8) and (3.9) are not for marginal posterior distributions, but for full conditional distributions of M_{na} . This is due to the fact that the marginal posterior distributions of U_n are analytically intractable.

3.6 Relationship with the telescoping sampling

In this section, we clarify the connection between the blocked Gibbs sampling and the telescoping sampling. The blocked Gibbs sampling is derived from the posterior distribution of a random measure induced by the Norm-IFPP, whereas the telescoping sampling is a partially marginalized algorithm constructed from the EPPF. Although the two methods arise from fundamentally different formulations, they share several similarities, including the sampling of M . To the best of our knowledge, their relationship has not been clarified so far, as both methods were proposed independently around the same time.

First, we explain that the blocked Gibbs sampling can be derived in a manner similar to the telescoping sampling scheme. Specifically, it can be derived from both the full mixture posterior $p(M, S, U_n, \tau_{1:M}, c \mid y)$ and the collapsed mixture posterior $p(M, \mathcal{C}, U_n, \tau_{1:k} \mid y)$, where $\mathcal{C} = \{\mathcal{C}_1, \dots, \mathcal{C}_k\}$ is a partition of $\{1, \dots, n\}$ into k blocks, where $|\mathcal{C}_i| = n_i$ for $i = 1, \dots, k$ and $\sum_{i=1}^k n_i = n$, and the hyperparameters ρ and η are omitted for simplicity. This full mixture posterior is used to sample $\tau_{1:M}$, c , S and U_n (Step 1, 2, 5, 6, 7 in

Algorithm 1). The collapsed mixture posterior is obtained by marginalizing out S , the unallocated parameters, and all assignments c that induce the same partition \mathcal{C} in the full mixture posterior. Thus, by Theorem 4.1 in Argiento and De Iorio (2022), the conditional distribution of M given $U_n = u, \mathcal{C}$ is

$$\mathbb{P}(M = m \mid \mathcal{C}, U_n = u) \propto \frac{m!}{(m-k)!} \psi(u)^{m-k} q_M(m), \quad m = k, k+1, \dots$$

This full conditional distribution of M is equivalent to the equation (2.7), shifted by k .

The latent variable U_n is essential distinction between the two methods, while the blocked Gibbs sampling shares many advantages with the telescoping sampling discussed in Frühwirth-Schnatter et al. (2021). In other words, the blocked Gibbs sampling can be regarded as a telescoping sampling augmented with the latent variable U_n . By this latent variable, the full conditional distribution M_{na} (or M) can be easily sampled when q_M is Poisson distribution or negative binomial distribution. This is a major advantage over the telescoping sampling, because, in practice, an upper bound M_{\max} is required and M is sampled from a multinomial distribution over $\{k, \dots, M_{\max}\}$ due to the complex form of M 's full conditional distribution.

3.7 Extended telescoping sampling

In this section, we extend the telescoping sampling so that it can be applied to model (2.3), thereby relaxing the Dirichlet restriction in Frühwirth-Schnatter et al. (2021).

The conditional distributions for \mathcal{C} , given $M = m$ and $U_n = u$, and for M , given $\mathcal{C}, U_n = u$ are required to construct our algorithm under (2.3).

Proposition 3.2. *Let $\mathcal{C} = \{\mathcal{C}_1, \dots, \mathcal{C}_k\}$ be a set partition with $n_j = |\mathcal{C}_j|$ and $\sum_{j=1}^k n_j = n$. Under (2.3), the EPPF is the following:*

$$p(\mathcal{C}) = \int_0^\infty \frac{u^{n-1}}{\Gamma(n)} \sum_{m=k}^\infty \frac{m!}{(m-k)!} \psi(u; m)^{m-k} \left\{ \prod_{j=1}^k \kappa(u; n_j, m) \right\} q_M(m) du, \quad (3.11)$$

where $\psi(u; m)$ and $\kappa(u; n, m)$ are the Laplace transform and cumulant of h_M , respectively.

Algorithm 2 Extended telescoping sampling

Step 3. Sample the hyperparameter η of the q_M from

$$p(\eta \mid \text{rest}) \propto p(\eta)q_M(m).$$

Step 3'. Sample the hyperparameter ρ of the h from

$$p(\rho \mid \text{rest}) \propto \left\{ \prod_{j=1}^k \kappa(u; n_j, m) \right\} \psi(u; m)^{m-k} p(\rho).$$

Step 4. Sample M from the following discrete distribution

$$\mathbb{P}(M = m \mid \text{rest}) \propto \frac{m!}{(m-k)!} \left\{ \prod_{j=1}^k \kappa(u; n_j, m) \right\} \psi(u; m)^{m-k} q_M(m), \quad m = k, k+1, \dots$$

Moreover, the conditional probability of $M = m$, for $m = k, k+1, \dots$, is proportional to the following:

$$\mathbb{P}(M = m \mid U_n = u, \mathcal{C}) \propto \frac{m!}{(m-k)!} \psi(u; m)^{m-k} \left\{ \prod_{j=1}^k \kappa(u; n_j, m) \right\} q_M(m). \quad (3.12)$$

From Proposition 3.2, the Algorithm 2 is immediately derived, showing only the parts that differ from Algorithm 1. If h_M is $\text{Gamma}(\gamma/M, 1)$ or $\text{IGau}(\alpha/M, 1)$, Algorithm 2 can be applied to the DMFM based on the Dirichlet and normalized inverse Gaussian distributions, respectively. The main difference from Algorithm 1 is that the Laplace transform and the cumulant of h_M depend on M . Since the full conditional distributions of M (or M_{na}) and the summation $\sum_{m=k}^{\infty} \frac{m!}{(m-k)!} \left\{ \prod_{j=1}^k \kappa(u; n_j, m) \right\} \psi(u; n_j, m)^{m-k} q_M(m)$ strongly depend on $\psi(u; m)$ and $\kappa(u; n, m)$, they cannot, in general, be expressed in a simple form. Thus, Step 3 in Algorithm 2 is replaced by sampling from the full mixture posterior, and M is not marginalized out in Step 3', as in Frühwirth-Schnatter et al. (2021). In addition, in Step 4, it is practically necessary to set an upper bound M_{\max} and sample from a multinomial distribution.

4 Empirical demonstrations

We evaluate the performance of the MFM-IGau and MFM-Ga methods through some numerical experiments. Recall that γ is the shape parameter of the prior distribution of unnormalized weights in the proposed method (MFM-IGau), while α is that of MFM-Ga.

4.1 Clustering performance

In this subsection, we compare the clustering performance of the proposed methods, MFM-IGau and DMFM-IGau, with MFM-Ga and DMFM-Ga, using artificial and real data.

4.1.1 Artificial data

In this simulation, we assume that $M_{\text{true}} = k_{\text{true}} = 8$, and data are generated from the following multivariate normal distribution mixture:

$$f(y \mid \mu_1, \dots, \mu_8) = \sum_{i=1}^8 w_i N_2(y \mid \mu_i, \sigma^2 I_2),$$

where $w_i = i^{-1.75} / \sum_{i=1}^8 w_i$, $\mu_1 = (2, 0)^\top$, $\mu_2 = (2, 5)^\top$, $\mu_3 = (6, 0)^\top$, $\mu_4 = (6, 5)^\top$, $\mu_5 = (10, 0)^\top$, $\mu_6 = (10, 5)^\top$, $\mu_7 = (14, 0)^\top$, $\mu_8 = (14, 5)^\top$, $\sigma^2 = 0.45$ and I_2 is the 2×2 identity matrix. We set $n = 50, 100, 200, 300, 400$ and generate 50 datasets for each n .

This data generating process represents a situation in which many mixture components have small weights, so that not all components necessarily contribute to the observed data. When n is small, it is difficult to obtain observations from all components, whereas as n increases, it becomes more likely that observations are obtained from every component.

MCMCs were run for 30,000 iterations, with the first 20,000 discarded as burn-in. We assume that $M - 1 \mid \Lambda \sim \text{Poisson}(\Lambda)$ and $\Lambda \sim \text{Gamma}(1, 0.1)$ and employ a multivariate normal kernel with a normal-inverse-Wishart hierarchical prior in Section 3.4.1, where $b_0 = \text{median}(y)$, $B_0 = \text{diag}(R_1^2, \dots, R_d^2)$, R_j is the range of data $y_{1:n}$ in j th dimension, $c_0 = 2.5 + (d - 1)/2$, $g_0 = 0.5 + (r - 1)/2$ and $G_0 = 100g_0/c_0 \text{diag}(1/R_1^2, \dots, 1/R_d^2)$. Also, we set shape parameters $\alpha, \gamma = 1.0$ for MFM-IGau, DMFM-IGau and MFM-Ga, and we

assume a prior F distribution $F(6, 3)$ to shape parameter DMFM-Ga as in Frühwirth-Schnatter et al. (2021).

To measure performance, we consider the posterior mean of the Adjusted Rand index (ARI) (Hubert and Arabie, 1985), which is a measure of the goodness of clustering. When it is close to 1, the assignment estimate is reasonable. The respective averages over 50 repetitions are denoted by $\widehat{\text{ARI}}$.

Overall, figure 2 shows that $\widehat{\text{ARI}}$ of all methods increase toward 1 as n becomes larger. MFM-IGau consistently attains higher clustering accuracy than MFM-Ga, and DMFM-IGau exhibits the best overall performance. Although the difference between DMFM-IGau and DMFM-Ga is small, DMFM-IGau does not incorporate learning for α . This result indicates that stable posterior inference is achieved due to the less informative nature of the normalized inverse Gaussian distribution.

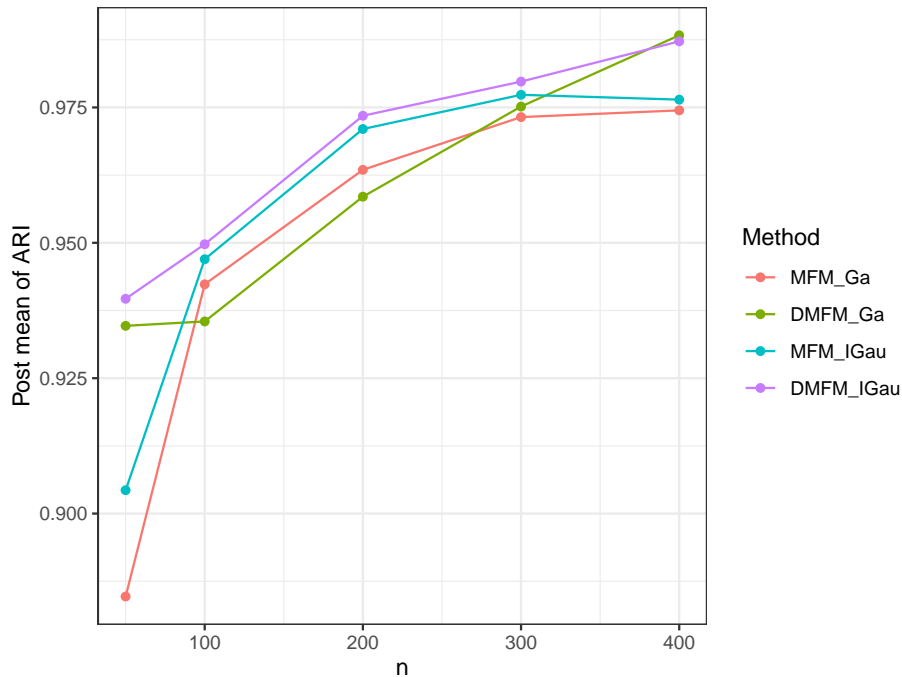


Figure 2: Line plots of the posterior mean of ARI averaged over 50 Monte Carlo replications for MFM-Ga, DMFM-Ga, MFM-IGau and DMFM-IGau.

4.1.2 Thyroid data

We apply the proposed method MFM-IGau and DMFM-IGau to famous thyroid data. The main purpose of this analysis is to infer the number of cluster k and the number of

components M and examine the impact of choice of q_M . The thyroid data are available from the R package `mclust` and is well known as benchmark data for clustering. The sample size is 215 and the dimension of the data is 6. The thyroid disease of each patient is included and classified into three categories: Normal, hypo and hyper. The number of diseases are 150, 30 and 35, respectively. Using these labels as true labels, the main interest is whether the number of components is estimated to be 3. We use priors Poisson distribution $\text{Poisson}(1)$, geometric distribution $\text{Geo}(0.1)$ and beta negative binomial distribution $\text{BNB}(1, 4, 3)$ for M , and F -distribution $F(6, 3)$ for α .

Table 1 shows that the posterior modes for MFM-IGau and DMFM-IGau are all equal to 3. These results are consistent with those obtained from DMFM-Ga. In addition, the table indicates that both the first and third quartiles are 3, and that the posterior probabilities of $M_{na} = 0$ are very close to 1. This implies that the difference between the posterior number of components and the posterior number of clusters obtained by MFM-IGau and DMFM-IGau is extremely small. Furthermore, the interquartile range of M is tighter than that reported in Frühwirth-Schnatter et al. (2021), providing stronger evidence that $M = 3$ under our proposed methods than under DMFM-Ga. In addition, the overall results do not depend on the choice of the prior q_M , as is the case for DMFM-Ga.

Table 1: Posterior summaries of k and M for the thyroid data. The leftmost values represent the posterior modes, the values in brackets denote the first and third quartiles, and the rightmost values correspond to the posterior probabilities of $M_{na} = 0$.

	$p(k \mid \text{data})$		
	Poi(1)	Geo(0.1)	BNB(1, 4, 3)
MFM-IGau	3 [3, 3]	3 [3, 3]	3 [3, 3]
DMFM-IGau	3 [3, 3]	3 [3, 3]	3 [3, 3]

	$p(M \mid \text{data})$								
	Poi(1)		Geo(0.1)		BNB(1, 4, 3)				
MFM-IGau	3	[3, 3]	0.997	3	[3, 3]	0.980	3	[3, 3]	1.000
DMFM-IGau	3	[3, 3]	0.993	3	[3, 3]	0.973	3	[3, 3]	0.986

4.2 Density estimation

In this section, we compare MFM-IGau and MFM-Ga using the Galaxy data. The aim of this analysis is to examine how sensitive the posterior distribution of k and the density estimation based on the predictive distribution are to the choice of shape parameters.

We used the famous galaxy dataset, which is a small data set consisting of 82 velocities (km/sec) of different galaxies. The data are widely used in nonparametric Bayesian statistics as a benchmark for density estimation and cluster analysis. The details and a more comprehensive analysis of the data were given in Roeder (1990) and Grün et al. (2022).

We set $M - 1 \mid \Lambda \sim \text{Poisson}(\Lambda)$ and $\Lambda \sim \text{Ga}(1, 1/5)$. We also employ the univariate normal kernel $N(y \mid \mu, \sigma^2)$, and the normal-inverse gamma conjugate prior in Section 3.4.1: $N(\mu \mid m_0, \sigma^2/\tau) \times \text{IG}(\sigma^2 \mid c_0, C_0)$ as the prior of the parameters in the kernel. Moreover, we assume that the prior of C_0 is $\text{Gamma}(d_0, D_0)$, and we set $m_0 = (\max(\text{data}) + \min(\text{data}))/2$, $d_0 = 0.2$, $D_0 = 10/(\max(\text{data}) + \min(\text{data}))^2$ as Richardson and Green (1997). The parameter τ controls the smoothness of the estimated density function. We assume that the prior of the smoothing parameter τ is $\text{Gamma}(w, W)$, where $w = 0.5$ and $W = 50$ as Escobar and West (1995). Parameters τ and C_0 should be carefully learned from the data, since density estimation is sensitive to their choice. MCMC was run for 100,000 iterations with a burn-in of 90,000. Each value of $\alpha = 1.0, 0.2, 10^{-1}, 10^{-2}, 10^{-3}$ is considered, and γ is set to $\gamma = \alpha$ in each case. Note that the first and second moments of $\text{IGau}(\alpha, 1)$ and $\text{Gamma}(\gamma, 1)$ are both equal to α and γ , respectively; thus, this corresponds to a moment-matching setting. We evaluated the result of density estimation and posterior probabilities of k for each shapes.

We show the estimated density functions using the posterior means in Figure 3. From the figure, it is observed that the shapes of the estimated densities using the MFM-IGau do not depend on the choice of the shape parameter α . However, results using the MFM-Ga method seem to be strongly influenced by the choice of the shape parameter γ . For $\gamma = 10^{-2}$ and 10^{-3} , MFM-Ga cannot capture two large peaks in the middle.

The number of clusters in the galaxy data has been reported as 5 or 6 in existing stud-

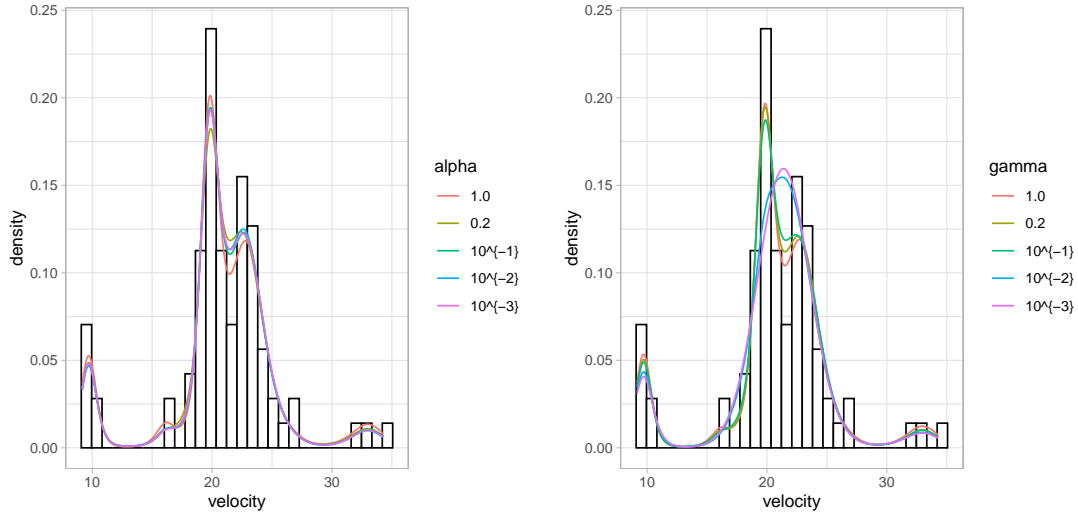


Figure 3: Results of density estimation for Galaxy data using MFM-IGau (left) and MFM-Ga (right).

ies. From Table 2, in MFM-IGau, the posterior distributions of k have large probabilities at $k = 5$ and 6 for all α , and the posterior distributions of k under MFM-IGau are more similar to each other across different value of α than those under MFM-Ga. Focusing on the number of clusters k , it is interesting that MFM-IGau is more robust than MFM-Ga with respect to the choice of the shape parameter in estimating k . This suggests that the prior distribution of k based on MFM-IGau is less informative than MFM-Ga, i.e., the same relationship holds for MFM-IGau and MFM-Ga as for normalized inverse Gaussian process and Dirichlet process.

The shape parameter of MFM-Ga should be chosen carefully because it has a significant impact on clustering, density estimation, and the appearance of empty components. However, MFM-IGau is much more robust than MFM-Ga with respect to the choice of the shape parameter. This is consistent with the earlier remark that the normalized inverse Gaussian distribution is less informative and more robust to parameter specification than the Dirichlet distribution, leading to more stable inference. Note that results do not differ substantially when information measures such as the expected Gini index are matched.

Table 2: Posterior probabilities of the number of clusters k for Galaxy data.

MFM-IGau								
	$k \leq 3$	$k = 4$	$k = 5$	$k = 6$	$k = 7$	$k = 8$	$k = 9$	$k \geq 10$
$\alpha = 1.0$	0.000	0.092	0.241	0.331	0.164	0.092	0.046	0.034
$\alpha = 0.2$	0.156	0.215	0.206	0.182	0.118	0.063	0.033	0.026
$\alpha = 10^{-1}$	0.089	0.127	0.214	0.224	0.169	0.094	0.052	0.031
$\alpha = 10^{-2}$	0.088	0.123	0.201	0.232	0.160	0.107	0.054	0.035
$\alpha = 10^{-3}$	0.082	0.152	0.256	0.221	0.143	0.081	0.039	0.025

MFM-Ga								
	$k \leq 3$	$k = 4$	$k = 5$	$k = 6$	$k = 7$	$k = 8$	$k = 9$	$k \geq 10$
$\gamma = 1.0$	0.044	0.120	0.232	0.236	0.188	0.104	0.044	0.033
$\gamma = 0.2$	0.145	0.198	0.304	0.186	0.098	0.040	0.019	0.009
$\gamma = 10^{-1}$	0.145	0.198	0.304	0.186	0.098	0.040	0.019	0.009
$\gamma = 10^{-2}$	0.775	0.195	0.024	0.005	0.000	0.000	0.000	0.000
$\gamma = 10^{-3}$	0.983	0.018	0.000	0.000	0.000	0.000	0.000	0.000

4.3 Community detection

We apply the proposed method to the community detection for network data. Similar comparisons as in Section 4.1 are made for both artificial and real data. Since the number of components of the finite mixture models is equivalent to the number of communities of the network, we use the same notation M to denote the number of communities.

4.3.1 Artificial data

First, we illustrate the performance of the proposed method using simulation data. We assume that the true number of communities and clusters is 2, denoted by $M_{\text{true}} = k_{\text{true}} = 2$ and the number of nodes in the network is set as $n = 50$. We generated 50 datasets under this setting. We here consider the balanced network, in that the true allocation consists of M_{true} communities with 25 nodes. For the true probability matrix Q , we assume that each component is expressed by $q_{rs} = q + (p - q)I(r = s)$, where $q = 0.1$, $p = 0.35$ and $1 \leq r \leq s \leq M_{\text{true}}$.

We use MFM-Geng, which is suggested by Geng et al. (2019) and equivalent to MFM-Ga, and DMFM-Ga as baseline methods. In MFM-Geng, γ is fixed at 1, and M is sampled by the post-preseeding step. We assign a BNB(1, 4, 3) prior to $M - 1$ and an $\mathcal{F}(6, 3)$ prior

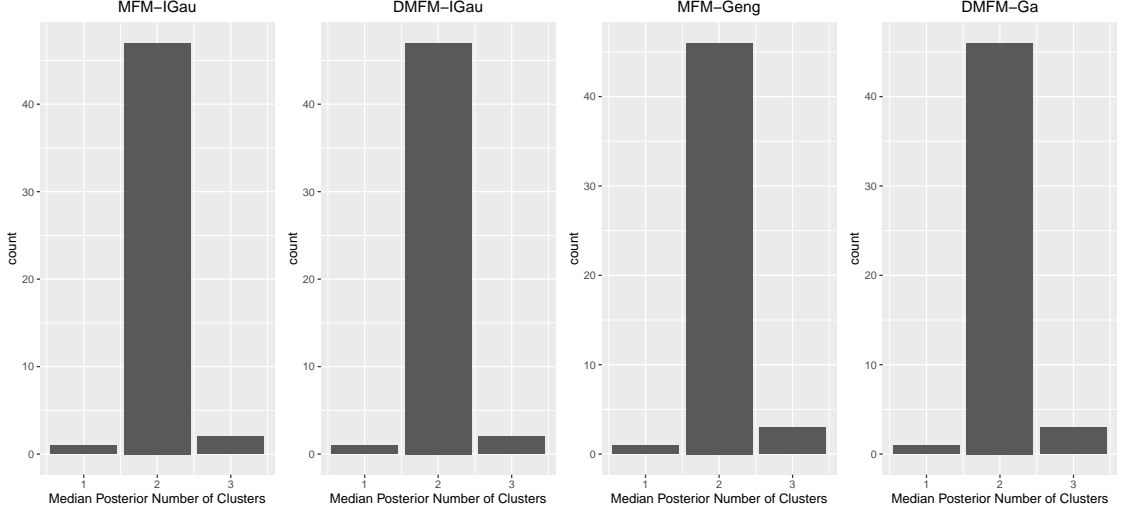


Figure 4: Bar plots of the posterior median number of clusters k . From left to right, the models are MFM-IGau, DMFM-IGau, MFM-Geng, DMFM-Ga.

to the shape parameters, employ (3.7) as a kernel and a prior, where $a_Q = 1$ and $b_Q = 1$.

We evaluate the performance in terms of $\widehat{\text{ARI}}$, $\widehat{\mathbb{P}}(M_{na} = 0)$ and the following two criteria:

- Modularity (Mod) (Newman and Girvan, 2004): This index measures the quality of the estimated community structure in a network. We computed this value based on the MAP estimate of the label c obtained by the method of Dahl (2009). We reported $\widehat{\text{Mod}}$, averaged over 50 replications.
- MCMC run times (seconds): All computations were implemented in R (version 4.4.0) on a laptop equipped with an Apple M2 chip (8-core CPU) and 16 GB of RAM, running macOS Sonoma 14.5. MCMCs were run for 100,000 iterations with a burn-in of 50,000 (no thinning).

From Figure 4 and the $\widehat{\text{ARI}}$ values in Table 3, the posterior estimates of k and the clustering accuracy are comparable across all methods. Although DMFM-Ga achieves a slightly higher ARI than the other methods, MFM-IGau and DMFM-IGau outperform MFM-Geng and DMFM-Ga in terms of modularity. This result indicates that MFM-IGau and DMFM-IGau better capture the community structures given the adjacency matrix. From the $\widehat{\mathbb{P}}(M_{na} = 0)$ values in Table 3, MFM-IGau and DMFM-IGau support $M = 2$ more tightly than the other methods. This result is also consistent with Proposition 3.1.

Table 3: Results of community detection over 50 simulated networks: $\widehat{\text{ARI}}$, $\widehat{\mathbb{P}}(M_{na} = 0)$, $\widehat{\text{Mod}}$, and MCMC run time (seconds). Standard deviations are given in parentheses.

	MFM-IGau	DMFM-IGau	MFM-Geng	DMFM-Ga
$\widehat{\text{ARI}}$	0.861 (0.090)	0.859 (0.084)	0.857 (0.083)	0.863 (0.087)
$\widehat{\text{Mod}}$	0.256 (0.055)	0.259 (0.053)	0.249 (0.068)	0.254 (0.060)
$\widehat{\mathbb{P}}(M_{na} = 0)$	0.988 (0.005)	0.976 (0.007)	0.938 (0.013)	0.908 (0.035)
MCMC run time (sec)	192.627 (18.252)	301.960 (29.480)	626.283 (33.969)	236.160 (22.320)

In Table 3, the most pronounced differences among the methods appear in terms of MCMC run time. MFM-IGau has the shortest run time, which can be attributed to the fact that all random numbers required at each step of the MCMC algorithm can be generated straightforwardly. DMFM-IGau and DMFM-Ga require more time than MFM-IGau, because sampling M from a multinomial distribution with an upper bound is necessary. DMFM-IGau is slower than DMFM-Ga, reflecting the greater complexity of the cumulant of the inverse Gaussian distribution compared with that of the gamma distribution. MFM-Geng takes by far the longest time for two reasons: label updates are based on a restaurant-process representation, and, as in DMFM-IGau and DMFM-Ga, M is sampled from a multinomial distribution with an upper bound.

4.3.2 Dolphins social network data

The dolphins social network is often used as a benchmark. Data can be obtained in <http://www-personal.umich.edu/mejn/netdata/>. The data is an undirected graph and expresses a small-scale animal social network with 64 bottlenose dolphins off Doubtful Sound, New Zealand. Each node represents a dolphin, and an edge is drawn if two dolphins appear to be closely related to each other. In previous studies, it is well-known that the network has two communities. The details of the data are found in Lusseau et al. (2003).

Table 4: Posterior summaries of k , M , and modularity for the dolphin data. The leftmost values represent the posterior modes, the values in brackets denote the 5% and 95% quantiles, and the rightmost values correspond to the posterior probabilities of $M_{na} = 0$.

	MFM-IGau	DMFM-IGau	MFM-Geng	DMFM-Ga
$p(k \mid \text{data})$	2 [2, 2]	2 [2, 2]	2 [2, 2]	2 [2, 2]
$p(M \mid \text{data})$	2 [2, 2] 0.988	2 [2, 2] 0.974	2 [2, 3] 0.954	2 [2, 3] 0.905
modularity	0.376	0.377	0.371	0.366

We compare the posterior distributions of the numbers of clusters and communities among MFM-IGau, DMFM-IGau, MFM-Geng, and DMFM-Ga. In addition, we construct a co-clustering matrix to quantify the uncertainty of clustering and compute the modularity value, which is calculated based on the MAP estimator derived by the method of Dahl (2009). In this analysis, we set $M - 1 \sim \text{Poisson}(1)$ and $a_Q = b_Q = 3.0$. From Table 4, although all the results for the number of clusters k are the same, the posterior distributions of M obtained from MFM-IGau and DMFM-IGau support $M = 2$ more strongly and more tightly than those obtained from MFM-Geng and DMFM-Ga. In addition, from the viewpoint of modularity, MFM-IGau and DMFM-IGau perform slightly better than MFM-Geng and DMFM-Ga. Finally, the co-clustering matrices obtained from MFM-IGau and DMFM-IGau are very similar to those from MFM-Geng, indicating that these methods produce reasonable clustering results.

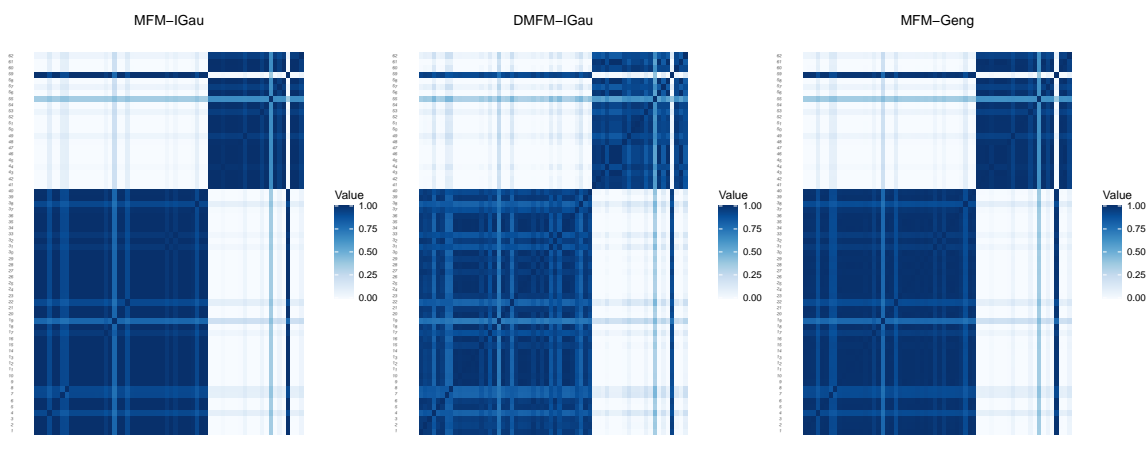


Figure 5: Co-clustering matrix with the MFM-IGau with $\alpha = 1.0$ (left) and the MFM-Geng with $\gamma = 1.0$ (right) for dolphins social network data.

5 Concluding remarks

We proposed MFM and DMFM based on the normalized inverse Gaussian distribution and constructed an efficient posterior sampling algorithm based on Argiento and De Iorio (2022) and Frühwirth-Schnatter et al. (2021). We illustrate the performance of the proposed method for clustering, density estimation, and community detection, compared to existing MFM and DMFM models based on the Dirichlet distribution.

The drawbacks of the proposed method are as follows. Some parameters involved in the model do not have closed-form marginal distributions because it is not easy to marginalize out U_n . For example, when we focus on clustering, obtaining the interpretable prior distribution for the number of clusters is very important (see e.g., Zito et al., 2024) to incorporate subjective prior information. However, the proposed model cannot lead to a tractable marginal prior distribution for the number of clusters. Also, MFM models consists of a distribution over a simplex based on the normalization of independent random variables. Therefore, the correlation between categories cannot be properly modeled. The normalized inverse Gaussian distribution has a negative covariance as well as the Dirichlet distribution. It may be inappropriate for data with positive correlations between categories, such as the proportion of symbiotic organisms present, disease complication data, or gene expression data. To address such a problem, it may be necessary to construct the MFM in a more general framework that removes the assumption of independence in the Norm-IFPP by Argiento and De Iorio (2022). The construction of MFMs using a more flexible distribution over a simplex that can also express positive correlations is an interesting future topic. Furthermore, the proposed model can be applied to spatial data (e.g., Geng et al., 2021), functional data (e.g., Hu et al., 2023) and network data with weighted edges, degree-corrected stochastic block models.

Acknowledgement

The authors would like to thank the editor, associate editor, and two anonymous referees for their careful reading and comments to improve the quality of this article. We also

thank Naoki Awaya for his valuable comments on an early revision of the manuscript. This work was supported by JST SPRING, Grant Number JPMJSP2132, and partially supported by the Japan Society for the Promotion of Science (grant number: 21K13835).

References

- Argiento, R., A. Cremaschi, and A. Guglielmi (2014). A “density-based” algorithm for cluster analysis using species sampling gaussian mixture models. *Journal of Computational and Graphical Statistics* 23(4), 1126–1142.
- Argiento, R. and M. De Iorio (2022). Is infinity that far? a bayesian nonparametric perspective of finite mixture models. *The Annals of Statistics* 50(5), 2641–2663.
- Dahl, D. B. (2009). Modal clustering in a class of product partition models.
- Escobar, M. D. and M. West (1995). Bayesian density estimation and inference using mixtures. *Journal of the American Statistical Association* 90(430), 577–588.
- Frühwirth-Schnatter, S. (2006). *Finite mixture and Markov switching models*. Springer.
- Frühwirth-Schnatter, S., G. Celeux, and C. P. Robert (2019). *Handbook of mixture analysis*. CRC press.
- Frühwirth-Schnatter, S. and S. Kaufmann (2008). Model-based clustering of multiple time series. *Journal of Business & Economic Statistics* 26(1), 78–89.
- Frühwirth-Schnatter, S., G. Malsiner-Walli, and B. Grün (2021). Generalized mixtures of finite mixtures and telescoping sampling. *Bayesian Analysis* 16(4), 1279–1307.
- Frühwirth-Schnatter, S. and S. Pyne (2010). Bayesian inference for finite mixtures of univariate and multivariate skew-normal and skew-t distributions. *Biostatistics* 11(2), 317–336.

- Geng, J., A. Bhattacharya, and D. Pati (2019). Probabilistic community detection with unknown number of communities. *Journal of the American Statistical Association* 114(526), 893–905.
- Geng, J., W. Shi, and G. Hu (2021). Bayesian nonparametric nonhomogeneous poisson process with applications to usgs earthquake data. *Spatial Statistics* 41, 100495.
- Green, P. J. (1995). Reversible jump markov chain monte carlo computation and bayesian model determination. *Biometrika* 82(4), 711–732.
- Greve, J., B. Grün, G. Malsiner-Walli, and S. Frühwirth-Schnatter (2022). Spying on the prior of the number of data clusters and the partition distribution in bayesian cluster analysis. *Australian & New Zealand Journal of Statistics* 64(2), 205–229.
- Grün, B., G. Malsiner-Walli, and S. Frühwirth-Schnatter (2022). How many data clusters are in the galaxy data set? bayesian cluster analysis in action. *Advances in data analysis and classification* 16(2), 325–349.
- Handcock, M. S., A. E. Raftery, and J. M. Tantrum (2007). Model-based clustering for social networks. *Journal of the Royal Statistical Society Series A: Statistics in Society* 170(2), 301–354.
- Holland, P. W., K. B. Laskey, and S. Leinhardt (1983). Stochastic blockmodels: First steps. *Social networks* 5(2), 109–137.
- Hu, G., J. Geng, Y. Xue, and H. Sang (2023). Bayesian spatial homogeneity pursuit of functional data: an application to the us income distribution. *Bayesian Analysis* 18(2), 579–605.
- Hubert, L. and P. Arabie (1985). Comparing partitions. *Journal of Classification* 2, 193–218.
- James, L. F., A. Lijoi, and I. Prünster (2009). Posterior analysis for normalized random measures with independent increments. *Scandinavian Journal of Statistics* 36(1), 76–97.

- Lijoi, A., R. H. Mena, and I. Prünster (2005). Hierarchical mixture modeling with normalized inverse-gaussian priors. *Journal of the American Statistical Association* 100(472), 1278–1291.
- Lusseau, D., K. Schneider, O. J. Boisseau, P. Haase, E. Sloaten, and S. M. Dawson (2003). The bottlenose dolphin community of doubtful sound features a large proportion of long-lasting associations: can geographic isolation explain this unique trait? *Behavioral Ecology and Sociobiology* 54, 396–405.
- McLachlan, G. (2000). Finite mixture models. *A wiley-interscience publication*.
- McLachlan, G. J., R. W. Bean, and D. Peel (2002). A mixture model-based approach to the clustering of microarray expression data. *Bioinformatics* 18(3), 413–422.
- McLachlan, G. J., S. X. Lee, and S. I. Rathnayake (2019). Finite mixture models. *Annual review of Statistics and its Application* 6(1), 355–378.
- Miller, J. W. (2023). Consistency of mixture models with a prior on the number of components. *Dependence Modeling* 11(1), 20220150.
- Miller, J. W. and M. T. Harrison (2018). Mixture models with a prior on the number of components. *Journal of the American Statistical Association* 113(521), 340–356.
- Newman, M. E. (2004). Detecting community structure in networks. *The European Physical Journal B* 38, 321–330.
- Newman, M. E. and M. Girvan (2004). Finding and evaluating community structure in networks. *Physical Review E* 69(2), 026113.
- Nobile, A. (1994). *Bayesian analysis of finite mixture distributions*. Carnegie Mellon University.
- Nobile, A. and A. T. Fearnside (2007). Bayesian finite mixtures with an unknown number of components: The allocation sampler. *Statistics and Computing* 17, 147–162.

Richardson, S. and P. J. Green (1997). On bayesian analysis of mixtures with an unknown number of components (with discussion). *Journal of the Royal Statistical Society Series B: Statistical Methodology* 59(4), 731–792.

Roeder, K. (1990). Density estimation with confidence sets exemplified by superclusters and voids in the galaxies. *Journal of the American Statistical Association* 85(411), 617–624.

Shi, J. and J. Malik (2000). Normalized cuts and image segmentation. *IEEE Transactions on Pattern Analysis and Machine Intelligence* 22(8), 888–905.

White, S. and P. Smyth (2005). A spectral clustering approach to finding communities in graphs. In *Proceedings of the 2005 SIAM international conference on data mining*, pp. 274–285. SIAM.

Zito, A., T. Rigon, and D. B. Dunson (2024). Bayesian nonparametric modeling of latent partitions via stirling-gamma priors. *Bayesian Analysis* 1(1), 1–28.

Appendix

A Proofs

A.1 Proof of the cumulant of IGau($\alpha, 1$)

Proof. We show by mathematical induction that the following equation holds.

$$(-1)^n \frac{d^n}{du^n} \psi(u) = \alpha^n \psi(u) \sum_{s=0}^{n-1} \frac{(n-1+s)!}{s!(n-1-s)!} (1+2u)^{-n/2-s/2} (2\alpha)^{-s}, \quad (\text{A.1})$$

where $\psi(u) = \exp(\alpha(1 - \sqrt{1+2u}))$, $u \geq 0$. If $n = 1$, the left side is $\alpha\psi(u)(1+2u)^{-1/2}$ and is equal to the right side. When $n = k$, we assume that (A.1) holds. We differentiate

both sides of (A.1) by u and $k + 1$ th derivative is

$$\alpha^{k+1}\psi(u)(1+2u)^{-k/2-1/2}\left(\sum_{s=0}^{k-1}A_s(1+2u)^{-s/2}(2\alpha)^{-s}+\sum_{s=0}^{k-1}B_s(1+2u)^{-s/2-1/2}(2\alpha)^{-s-1}\right),$$

where

$$A_s=\frac{(k-1+s)!}{s!(k-1-s)!},\quad B_s=\frac{2(k+s)!}{s!(k-1-s)!},\quad s=0,1,\dots,k-1.$$

$B_{k-1}=(2k)!/k!$ and

$$\begin{aligned}\sum_{s=0}^{k-1}B_s(1+2u)^{-s/2-1/2}(2\alpha)^{-s-1}&=\sum_{s=0}^{k-2}B_s(1+2u)^{-s/2-1/2}(2\alpha)^{-s-1}+\frac{(2k)!}{k!}(1+2u)^{-k/2}(2\alpha)^{-k}\\&=\sum_{s=1}^{k-1}B_{s-1}(1+2u)^{-s/2}(2\alpha)^{-s}+\frac{(2k)!}{k!}(1+2u)^{-k/2}(2\alpha)^{-k}.\end{aligned}$$

For $s=1,\dots,k-1$,

$$A_s+B_{s-1}=\frac{(k+s)!}{s!(k-s)!}$$

holds. Thus,

$$\begin{aligned}&\sum_{s=0}^{k-1}A_s(1+2u)^{-s/2}(2\alpha)^{-s}+\sum_{s=0}^{k-1}B_s(1+2u)^{-s/2-1/2}(2\alpha)^{-s-1}\\&=1+\sum_{s=1}^{k-1}(A_s+B_{s-1})(1+2u)^{-s/2}(2\alpha)^{-s}+\frac{(2k)!}{k!}(1+2u)^{-k/2}(2\alpha)^{-k}\\&=\sum_{s=0}^k\frac{(k+s)!}{s!(k-s)!}(1+2u)^{-s/2}(2\alpha)^{-s}.\end{aligned}$$

(A.1) are derived by this equation, when $n=k+1$. Let $K_\nu(z)$ be a modified Bessel function of the second kind. In general,

$$K_{n+1/2}(z)=K_{1/2}(z)\times\sum_{s=0}^n\frac{(n+s)!}{s!(n-s)!}(2z)^{-s}.$$

Therefore, (A.1) holds. □

A.2 Proof of Proposition 3.1

Proof. When $m \neq 0$,

$$\mathbb{P}(M_{na} = m \mid U_n = u, k, \Lambda) = \frac{k}{\Lambda\psi(u) + k} \mathcal{P}_0(m; \Lambda\psi(u)) + \frac{\Lambda\psi(u)}{\Lambda\psi(u) + k} \mathcal{P}_1(m; \Lambda\psi(u)).$$

Thus, the conditional expectation of M_{na} is

$$\begin{aligned} \mathbb{E}[M_{na} \mid U_n = u, k, \Lambda] &= \frac{k}{\Lambda\psi(u) + k} \times \Lambda\psi(u) + \frac{\Lambda\psi(u)}{\Lambda\psi(u) + k} \times (\Lambda\psi(u) + 1) \\ &= \Lambda\psi(u) \left(1 + \frac{1}{\Lambda\psi(u) + k} \right). \end{aligned}$$

Furthermore,

$$\begin{aligned} \mathbb{E}[M_{na} \mid U_n = u, k] &= \mathbb{E}_\Lambda[\mathbb{E}[M_{na} \mid U_n = u, k, M = m, \Lambda]] \\ &= \int \left(\Lambda\psi(u) \left(1 + \frac{1}{\Lambda\psi(u) + k} \right) \right) \frac{b_\Lambda^{a_\Lambda}}{\Gamma(a_\Lambda)} \Lambda^{a_\Lambda-1} \exp(-b_\Lambda \Lambda) d\Lambda \\ &\leq \psi(u) \times \frac{a_\Lambda}{b_\Lambda} + \frac{\psi(u)}{k} \times \frac{a_\Lambda}{b_\Lambda} \\ &= \psi(u) \times \frac{a_\Lambda}{b_\Lambda} \left(1 + \frac{1}{k} \right). \end{aligned}$$

Finally, the result follows from Markov's inequality. \square

A.3 Equivalence of Blocked Gibbs Sampler and Telescoping Sampler

In this section, we show that the blocked Gibbs sampler is essentially equivalent to the telescoping sampler. Our strategy is to derive the computational algorithm under the framework of (2.1) or (2.4) in the same manner as the telescoping sampler. To this end, we require the EPPF induced by the Norm-IFPP, which is given below.

Theorem A.1 (Theorem 4.1 in Argiento and De Iorio (2022)). *Let $\mathcal{C} = \{\mathcal{C}_1, \dots, \mathcal{C}_k\}$ be a partition of $\{1, \dots, n\}$ into k blocks, where $|\mathcal{C}_i| = n_i$ for $i = 1, \dots, k$ and $\sum_{i=1}^k n_i = n$.*

The EPPF $p(\mathcal{C})$ induced under (2.1) or (2.4) is

$$p(\mathcal{C}) = \int_0^\infty \frac{u^{n-1}}{\Gamma(n)} \Psi(u; k) \left\{ \prod_{j=1}^k \kappa(u; n_j) \right\} du,$$

where,

$$\Psi(u; k) = \sum_{m=0}^{\infty} \frac{(m+k)!}{m!} \psi(u)^m q_M(m+k).$$

Note that, for simplicity, we omit the hyperparameter η of q_M and the hyperparameter ρ of h . The full mixture posterior $p(M, S, \tau_{1:M}, c \mid y)$ is

$$p(M, S, \tau, c \mid y) \propto \frac{1}{T^n} \left\{ \prod_{m \in \mathcal{M}_a} S_m^{n_m} h(S_m) f(y^{[n_m]} \mid \tau_m) p_0(\tau_m) \right\} \left\{ \prod_{m \in \mathcal{M}_{na}} h(S_m) p_0(\tau_m) \right\} q_M(M),$$

where $y^{[n_m]}$ denotes the n_m observations belonging to the m th cluster \mathcal{C}_m . Also,

$$U_n \mid T \sim \text{Gamma}(n, T), \quad \frac{\Gamma(n)}{T^n} = \int_0^\infty e^{-Tu} u^{n-1} du.$$

Using the data augmentation with U_n , we obtain the following:

$$\begin{aligned} p(M, S, U_n, \tau_{1:M}, c \mid y) &\propto \frac{U_n^{n-1}}{\Gamma(n)} \left\{ \prod_{m \in \mathcal{M}_a} f(y_j^{[n_m]} \mid \tau_m) p_0(\tau_m) \right\} \left\{ \prod_{m \in \mathcal{M}_a} S_m^{n_m} \exp(-S_m U_n) h(S_m) \right\} \\ &\times \left\{ \prod_{m \in \mathcal{M}_{na}} \exp(-S_m U_n) h(S_m) \right\} q_M(M). \end{aligned}$$

Marginalizing out the empty components, S_1, \dots, S_M , and all allocations c that induce the same partition \mathcal{C} yields the following expression for $p(M, \mathcal{C}, U_n, \tau_{1:k} \mid y)$:

$$p(M, \mathcal{C}, U_n, \tau_{1:k} \mid y) \propto \left\{ \prod_{m \in \mathcal{M}_a} f(y_j^{[n_m]} \mid \tau_m) p_0(\tau_m) \right\} p(\mathcal{C}, U_n \mid M) q_M(M).$$

From Theorem A.1,

$$p(M, \mathcal{C}, U_n, \tau_{1:k} \mid y) \propto U_n^{n-1} \left\{ \prod_{m \in \mathcal{M}_a} f(y_j^{[n_m]} \mid \tau_m) p_0(\tau_m) \right\} \frac{M!}{(M-k)!} \left\{ \prod_{j=1}^k \kappa(n_j; U_n) \right\} \psi(U_n)^{M-k} q_M(M).$$

Therefore, we obtain

$$\mathbb{P}(M = m \mid \mathcal{C}, U_n = u) \propto \frac{m!}{(m-k)!} \psi(u)^{m-k} q_M(m), \quad m = k, k+1, \dots$$

The extended telescoping sampler is immediately obtained in the same manner by applying Proposition 3.2.

A.4 Proof of Proposition 3.2

Proof. This proposition follows from a slight modification of the proof of Theorem A.1, with most steps carrying over directly. Let $\mathcal{A}(\mathcal{C})$ be the set of all labels c that induces partition \mathcal{C} , and c_1^*, \dots, c_k^* be unique values of c . The EPPF $p(\mathcal{C})$ is written by $p(\mathcal{C}) = \sum_{m=1}^{\infty} p(\mathcal{C} \mid M = m) q_M(m)$, since $q_M(0) = 0$. Moreover,

$$\begin{aligned} p(\mathcal{C} \mid M = m) &= \mathbb{1}_{\{k \leq m\}} \sum_{c \in \mathcal{A}(\mathcal{C})} p(c \mid M = m) \\ &= \mathbb{1}_{\{k \leq m\}} \sum_{c \in \mathcal{A}(\mathcal{C})} \int p(c \mid \pi, M = m) p(\pi \mid M = m) d\pi \\ &= \mathbb{1}_{\{k \leq m\}} \sum_{c \in \mathcal{A}(\mathcal{C})} \mathbb{E} \left[\prod_{j=1}^k \pi_{c_j^*}^{n_j} \right]. \end{aligned}$$

Note that $\pi_{c_j^*}^{n_j} = (S_{c_j^*}/T)^{n_j}$ and $\Gamma(n) = T^n = \int_0^{\infty} e^{-Tu} u^{n-1} du$. Thus,

$$\begin{aligned} \mathbb{E} \left[\prod_{j=1}^k \pi_{c_j^*}^{n_j} \right] &= \mathbb{E} \left[\frac{1}{T^n} \prod_{j=1}^k S_{c_j^*}^{n_j} \right] \\ &= \int_0^{\infty} \frac{u^{n-1}}{\Gamma(n)} \left\{ \prod_{j=1}^k \int_0^{\infty} S_{c_j^*}^{n_j} e^{-S_{c_j^*} u} h_M(S_{c_j^*}) dS_{c_j^*} \right\} \left\{ \prod_{t \notin \{c_1^*, \dots, c_k^*\}} \int_0^{\infty} e^{-St} h_M(S_t) dS_t \right\} du \\ &= \int_0^{\infty} \frac{u^{n-1}}{\Gamma(n)} \left\{ \prod_{j=1}^k \mathbb{E} \left[S_{c_j^*}^{n_j} e^{-S_{c_j^*} u} \right] \right\} \left\{ \prod_{t \notin \{c_1^*, \dots, c_k^*\}} \mathbb{E} \left[e^{-St} \right] \right\} du \\ &= \int_0^{\infty} \frac{u^{n-1}}{\Gamma(n)} \left\{ \prod_{j=1}^k \kappa(u; n_j, m) \right\} \psi(u; m)^{m-k} du, \end{aligned}$$

where, if $M = m$, $\psi(u; m) = \int_0^\infty e^{-uS} h_M(S) dS$ and $\kappa(u; n, m) := (-1)^n \frac{d^n}{du^n} \psi(u; m) = \int_0^\infty S^n e^{-Su} h_M(S) du$. Here, if $M = m$, we have

$$\#\mathcal{A}(\mathcal{C}) = \frac{m!}{(m-k)!k!} \times k! = \frac{k!}{(m-k)!}.$$

Therefore,

$$\begin{aligned} p(\mathcal{C}) &= \sum_{m=1}^{\infty} p(\mathcal{C} \mid M = m) q_M(m) \\ &= \sum_{m=1}^{\infty} \mathbb{1}_{\{k \leq m\}} \frac{m!}{(m-k)!} \int_0^\infty \left\{ \prod_{j=1}^k \kappa(u; n_j, m) \right\} \psi(u; m)^{m-k} du \\ &= \sum_{m=k}^{\infty} \frac{m!}{(m-k)!} \int_0^\infty \left\{ \prod_{j=1}^k \kappa(u; n_j, m) \right\} \psi(u; m)^{m-k} du \\ &= \int_0^\infty \frac{u^{n-1}}{\Gamma(n)} \Omega(u; k) du, \end{aligned}$$

where,

$$\Omega(u; k) := \sum_{m=k}^{\infty} \frac{m!}{(m-k)!} \psi(u; m)^{m-k} \left\{ \prod_{j=1}^k \kappa(u; n_j, m) \right\} q_M(m+k).$$

Finally, the conditional distribution of M is derived from the collapsed mixture posterior as follows:

$$\begin{aligned} p(M, \mathcal{C}, u, \tau_{1:k} \mid y) &\propto \left\{ \prod_{m \in \mathcal{M}_a} f(y_j^{[n_m]} \mid \tau_m) p_0(\tau_m) \right\} p(\mathcal{C}, u \mid M) q_M(M) \\ &\propto \left\{ \prod_{m \in \mathcal{M}_a} f(y_j^{[n_m]} \mid \tau_m) p_0(\tau_m) \right\} \frac{m!}{(m-k)!} \left\{ \prod_{j=1}^k \kappa(u; n_j, m) \right\} \psi(u; m)^{m-k} q_M(M) \\ \mathbb{P}(M = m \mid U_n = u, \mathcal{C}) &\propto \frac{m!}{(m-k)!} \psi(u; m)^{m-k} \left\{ \prod_{j=1}^k \kappa(u; n_j, m) \right\} q_M(m). \end{aligned}$$

□

B Additional simulation results

B.1 Gini Index Comparison

In this section, we compare the Dirichlet distribution and the normalized inverse Gaussian distribution in terms of *Gini index*.

Let x be a d -dimensional vector on \mathbb{S}_d . We define the Gini index of x as

$$G(x) = \sum_{i=1}^d x_i(1 - x_i).$$

This measure indicates that when $G(x)$ is small, the point x lies near a vertex or an edge of the simplex, whereas when $G(x)$ is large, the point x lies near the barycenter of the simplex.

We examine the expected values of the Gini index for (symmetry) Dirichlet and normalized inverse Gaussian distribution. Let $\pi = (\pi_1, \dots, \pi_d) \sim \text{NIGau}(\alpha, \dots, \alpha)$. From Proposition 2 in Lijoi et al. (2005),

$$\mathbb{E}[\pi_i] = \frac{1}{d}, \quad \text{Var}[\pi_i] = \alpha^2(d-1)e^{d\alpha}\Gamma(-2, d\alpha), \quad i = 1, \dots, d,$$

where $\Gamma(\cdot, \cdot)$ is the incomplete gamma function. Thus, we obtain immediately,

$$\mathbb{E}[G(\pi)] = 1 - \frac{1}{d} - d\alpha^2(\alpha-1)e^{d\alpha}\Gamma(-2, d\alpha).$$

From Figure 6, values of the Dirichlet distribution decreases sharply as the parameter approaches the origin. In contrast, that of the normalized inverse Gaussian distribution decline much more gradually. This corresponds to the fact that, for the Dirichlet distribution with a small γ , the probability mass tends to concentrate on the vertices or edges of the simplex. In contrast, even when α is small, the normalized inverse Gaussian distribution does not induce the same sparsity as the Dirichlet distribution, resulting in a more dispersed distribution over the simplex. Therefore, in settings such as the DMFM where the shape parameters naturally become small, using the normalized inverse Gaus-

sian distribution can lead to more stable posterior inference.

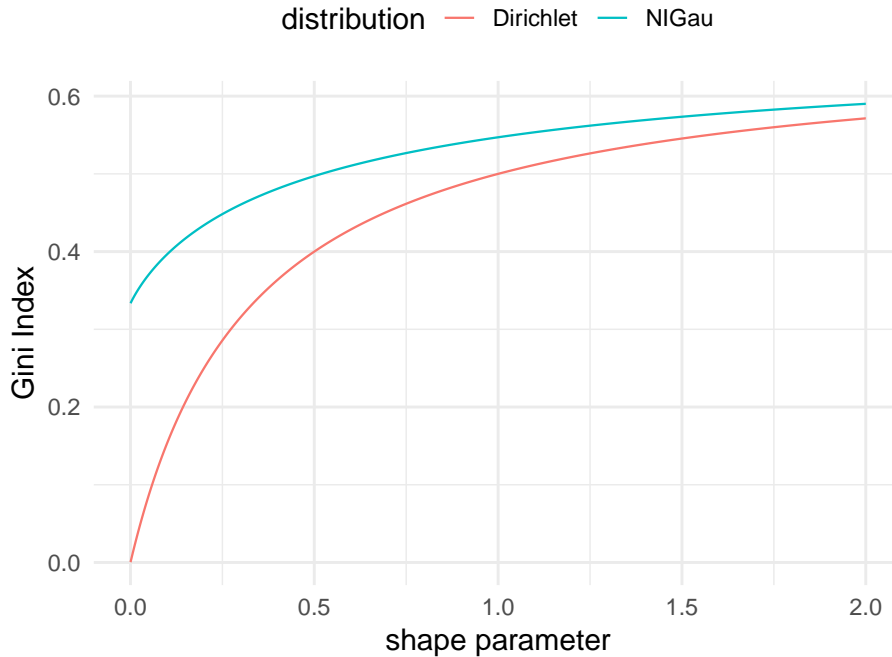


Figure 6: $\mathbb{E}[G(\pi)]$ for $\text{Dirichlet}(\gamma, \gamma, \gamma)$ and $\text{NIGau}(\alpha, \alpha, \alpha)$. These values were computed on a grid of 10000 points between 0 and 2 (excluding 0).

B.2 Additional Numerical Experiment

We conduct numerical experiments for MFM-IGau and MFM-Ga by matching moments and $\mathbb{E}[G(\pi)]$, focusing on the inference of the number of components. We assume that $M_{\text{true}} = k_{\text{true}} = 3$, and data are generated from the following:

$$f(y \mid \mu_1, \mu_2, \mu_3) = \sum_{i=1}^3 w_i N_2(y \mid \mu_i, \sigma^2 I_2),$$

where $w_i = 1/3$, $\mu_1 = (2, 0)^\top$, $\mu_2 = (2, 5)^\top$, $\mu_3 = (6, 0)^\top$, $\sigma^2 = 0.45$ and I_2 is the 2×2 identity matrix. We set $n = 300$ and generate 50 datasets. We set $\alpha = 0.1, 0.01, 0.001$ and consider the following two settings for γ :

- Moment match: We set $\gamma = 0.1, 0.01, 0.001$. Note that first and second moments of $\text{Gamma}(\gamma)$ and $\text{IGau}(\alpha, 1)$ are γ and α , respectively.
- $\mathbb{E}[G(\pi)]$ match: We set $\gamma = 0.490, 0.352, 0.335$. For each α , we compute $\mathbb{E}[G(\pi)]$ for

$\text{NIGau}(\alpha, \alpha, \alpha)$ and determine the corresponding value of γ for each α , using the `uniroot` function in R.

The remaining settings for kernels are the same as in Section 4.1.1. Each MCMC iteration is 30000 and the first 20000 samples are not used as a burn-in period. We assume that $M - 1 \mid \Lambda \sim \text{Poisson}(\Lambda)$ and $\Lambda \sim \text{Gamma}(1, 1)$.

In Table 5, we reported posterior probabilities averaged over 50 repetitions. We observe that MFM-IGau consistently yields the highest (averaged) posterior probability at $M = 3$. On the other hand, in the moment match case, MFM-Ga tends to overestimate M , because it produces many empty components when γ is small. In the Gini index match case, MFM-Ga also assigns the highest posterior probability to $M = 3$, similarly to MFM-IGau, but the probability is lower than that of MFM-IGau. Moreover, the results for very small γ , such as $\gamma = 0.1, 0.01, 0.001$, could also be interpreted from the perspective of the Gini index. When γ is extremely small, the expected Gini index tends to decrease, and consequently the Dirichlet prior assigns very small probabilities to many components. Consequently, this prior structure may generate unnecessary empty components.

Table 5: Posterior probabilities and their standard deviations (shown in parentheses) of the number of components M averaged over 50 Monte Carlo replications. The highest value is bolded.

MFM-IGau									
	$M = 1$	$M = 2$	$M = 3$	$M = 4$	$M = 5$	$M = 6$	$M = 7$	$M = 8$	$M \geq 9$
$\alpha = 10^{-1}$	0.000 (0.000)	0.000 (0.000)	0.971 (0.059)	0.024 (0.046)	0.004 (0.021)	0.001 (0.003)	0.000 (0.000)	0.000 (0.000)	0.000 (0.000)
$\alpha = 10^{-2}$	0.000 (0.000)	0.000 (0.000)	0.959 (0.063)	0.036 (0.054)	0.004 (0.008)	0.001 (0.004)	0.000 (0.002)	0.000 (0.001)	0.000 (0.000)
$\alpha = 10^{-3}$	0.000 (0.000)	0.000 (0.000)	0.941 (0.111)	0.048 (0.096)	0.007 (0.014)	0.002 (0.006)	0.001 (0.003)	0.000 (0.002)	0.001 (0.003)

MFM-Ga									
	$M = 1$	$M = 2$	$M = 3$	$M = 4$	$M = 5$	$M = 6$	$M = 7$	$M = 8$	$M \geq 9$
$\gamma = 10^{-1}$	0.000 (0.000)	0.000 (0.000)	0.331 (0.100)	0.301 (0.021)	0.187 (0.035)	0.098 (0.028)	0.047 (0.017)	0.021 (0.009)	0.016 (0.009)
$\gamma = 10^{-2}$	0.000 (0.000)	0.000 (0.000)	0.098 (0.021)	0.172 (0.024)	0.187 (0.013)	0.165 (0.005)	0.128 (0.009)	0.091 (0.012)	0.159 (0.037)
$\gamma = 10^{-3}$	0.000 (0.000)	0.000 (0.000)	0.066 (0.003)	0.131 (0.004)	0.161 (0.004)	0.159 (0.004)	0.136 (0.003)	0.107 (0.003)	0.240 (0.009)
$\gamma = 0.490$	0.000 (0.000)	0.000 (0.000)	0.798 (0.070)	0.170 (0.048)	0.028 (0.019)	0.004 (0.005)	0.001 (0.001)	0.000 (0.000)	0.000 (0.000)
$\gamma = 0.352$	0.000 (0.000)	0.000 (0.000)	0.717 (0.040)	0.221 (0.024)	0.050 (0.012)	0.010 (0.004)	0.002 (0.001)	0.000 (0.000)	0.000 (0.000)
$\gamma = 0.335$	0.000 (0.000)	0.000 (0.000)	0.693 (0.053)	0.237 (0.030)	0.056 (0.016)	0.012 (0.005)	0.002 (0.001)	0.000 (0.000)	0.000 (0.000)